https://erjm.journals.ekb.eg
ISSN: 1110-1180

DOI: ---------

ERJ
Engineering Research Journal
Faculty of Engineering
Menoufia University

Theoretical Investigation of Passive Horse-Shoe Vortex

Tarek A. Ghonim and Ibrahim O. Elhag Ali

Department of Mechanical Power Eng., Faculty of Eng., Menoufia University, Egypt.
(Corresponding author: tarek_ghonim@sh-eng.menofia.edu.eg)

ABSTRACT
This paper investigates a new method to eliminate the Horse-Shoe Vortex (HSV). It involves creating a thorough hole at the base of the cylinder where the HSV is formed. CFD simulation was conducted using ANSYS 15.2, and the results were compared and analyzed with and without the presence of the hole. Different speeds of the upstream flow without the hole and different hole heights were investigated. The minimum effective height that eliminated completely the HSV was determined. The qualitative analysis of CFD results showed that the HSV was eliminated totally at certain ranges of the dimensions of the hole.

Keywords: *Horse-Shoe Vortex; passive elimination; junction flow; CFD.*

1. Introduction

Energy issue is one of the most demanding issues worldwide, rich and poor nations are concerned about their energy share and many countries are trying very hard to save its energy resources to the utmost level. Two of the main consumers of the world energy are transportation and energy generation, so any tiny improvement in the efficiency of either process will save so much energy and money.

Secondary flows are important contributors to energy degradation in many devices. One of these secondary flows is the Horse-Shoe Vortex (HSV) which is found in airplanes, turbomachines and many other applications.

HSV forms when the main flow meets an obstacle, the velocity distribution of the main flow, whether laminar or turbulent, starts at zero value adjacent to the wall as to the no-slip condition then increases through the boundary layer thickness to the free stream velocity. In case of flow over a flat plate, the static pressure does not change with height as stated in Prandtl's assumptions of the Boundary Layer (BL), but the dynamic pressure changes due to the variation in the velocity within BL. When the main flow meets an obstacle the dynamic pressure starts with zero value at the corner of the junction with the flat plate and the obstacle then increases in the vertical direction as the velocity increases. Fluid motion takes place because of the change in total pressure, which is higher outside BL than within BL. So a secondary stream of flow moves downwards along the vertical direction of the obstacle then hits the flat plate and still have higher momentum than the upstream fluid, which has low momentum as to the dissipation in BL. This secondary stream of the fluid moves upstream until its momentum is dead. When the recirculated stream is hit by the upstream flow, it splits into two minor streams around the obstacle making a shape like a horseshoe, which is HSV. In all, the interaction of the BL of the flow developing on a surface and an obstacle fixed to the surface results in the HSV [1], these conditions can be found in wing-fuselage junction in airplanes, blade-hub junction in turbomachines and many other applications.

The development of HSV results in higher wall shear stress as to the intense mixing, which causes high momentum flow to be introduced from the freestream to the boundary layer. This leads to an increase in the dissipation of energy and losses, so a total or a partial elimination of HSV reduces energy degradation in applications like airplanes and turbomachinery, instead increasing HSV intensity helps in heat transfer enhancement, [2].

On the contrary HSV is used as a mean to enhance heat transfer on the gas-side in compact heat exchangers. In [3, 4] heat transfer is modified using surface topology alteration which in turn modifies the HSV structure and also heat transfer. Simpson [5] performed a detailed review on junction flows considering the HSV. While Devenport and Simpson [6] made another study showing the bimodal nature of the HSV by investigating time-dependent and time-averaged turbulence structure near the nose of a wing-body junction. The literature is full of studies that attempted to reduce the strength of HSV or eliminate it whether passively or actively. Devenport et al. [7] examined the effects of a

constant-radius circular concave fillet near the blade vertex, which was found not effective to prevent the formation of the HSV, instead it causes HSV to form away from the wing. Also, Kubendran et al. [8] performed experiments on leading-edge swept fairings by considering turbulent flow around a wing/fuselage-type juncture. K. Kang et al. [9] used an upstream cavity to increase the momentum within the BL to face the recirculated flow and found that only one vortex formed instead of a set of vortices. Philips et al. [10] and D. Barberis et al. [11] used suction to eliminate HSV in which the BL, which is the main source of HSV, was sucked. It was found to be far more effective than other passive techniques discussed before but the optimum suction flow rate must be determined to optimize the total cost of the process.

2. Gap Analysis

As can be seen from literature review available, that the passive methods used to reduce the HSV intensity are many like using fences, fillets of different shapes and cavities but none of them managed to eliminate the HSV totally.

The present study is associated with a novel way to passively eliminate the HSV by making a thorough duct (hole) through the obstacle at the junction region, different heights of the hole were examined.

3. Methodology

This section contains the research methods in the following order:

3.1 Geometry

The model consists of a cylinder of 50 mm diameter and 150 mm height. The cylinder is contained in a duct of 150 mm height, 300mm width and stream-wise length of 450 mm. The distance upstream of the cylinder is 160 mm and downstream the cylinder is 240 mm.

As the solution is steady, it is favorable to make use of computational similarity, so half of the fluid domain is used to save computational time. The half of the solid cylinder is subtracted from the duct to result in the fluid (air) domain as shown in Fig. (1).

The modification in the geometry is to tunnel a thorough hole of width 10 mm and variable height through the cylinder, in Fig. (2).

It could be seen in the literature that steady and unsteady analysis of the HSV used the symmetry plane of the obstacle (cylinder in current case) as the main plane to show the HSV and the illustrated modifications.

In current study, the symmetry plane is used to validate the model and to show the effect of the hole presence on the HSV structure. Along the vertical red line shown in Fig. (3), upstream of the cylinder the u-velocity (velocity in x- direction) is computed using ANSYS post processing tool to see whether circulation of the flow takes place or not, if circulation takes place the u-velocity will be negative. The magnitude of the negative u-velocity is an indicative value of the intensity of the HSV.

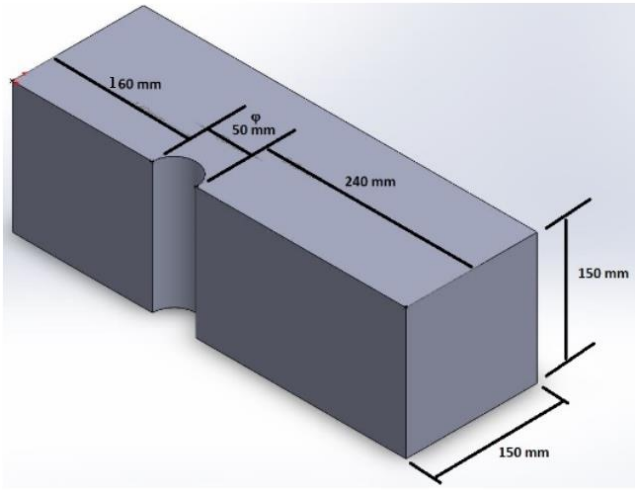

Fig. (1) Dimensions of the fluid domain (half of the physical domain)

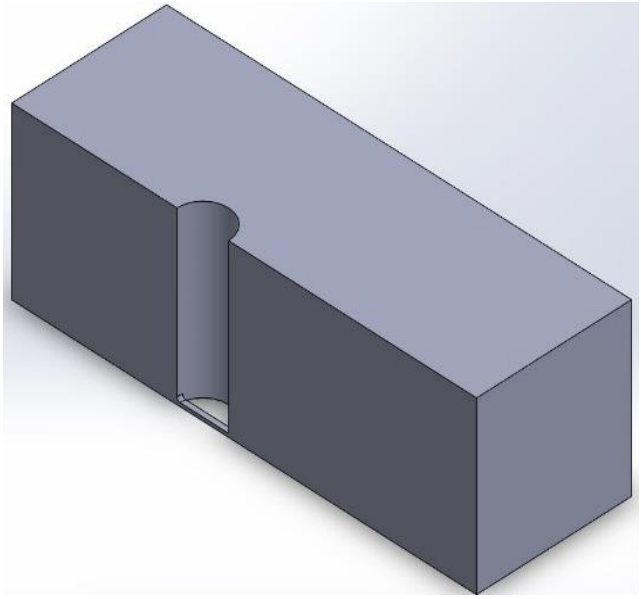

Fig. (2) The fluid domain with the modification (a thorough hole is made at the center of the cylinder)

3.2 Grid independence study

As for the case without a hole, 578254, 958745 and 1547896 elements were used. The suitability of the grid is determined based on the ability of the mesh to

capture the finest details of the HSV structure. It was found that the 958745 and 1547896 had very close HSV structure in the symmetry plane and very close to the experimental validation. So the 958745 was .selected to save computational time

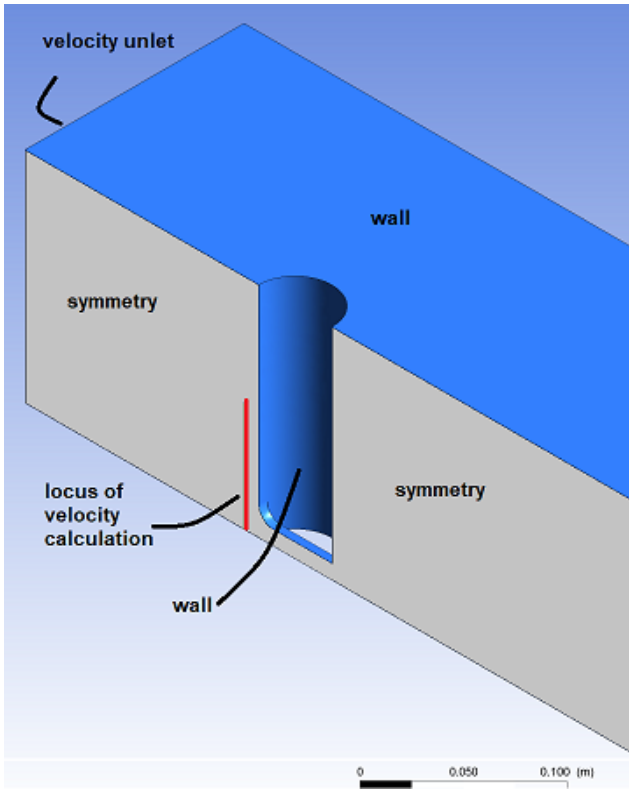

Fig. (3) The boundary conditions and the locus of u-velocity calculation

For the case with a hole, the degree of refinement required is higher so many refinement zones were used (which is illustrated in the mesh section below) to adapt the average skewness and aspect ratio to avoid divergence, and about 2.2 million cells were implemented.

3.3 Mesh

The meshing of the fluid domain with the hole is shown in Fig. (4). Four different refinement zones were implemented to get to the finest details of the phenomena especially around the corner. As for the boundary layer, 15 inflation layers are used with first layer thickness of 0.02 mm to get Y^+ values less than one allover the domain which is a condition in SST turbulence model. The average skewness is about 0.2 and the average aspect ratio is 17.843.

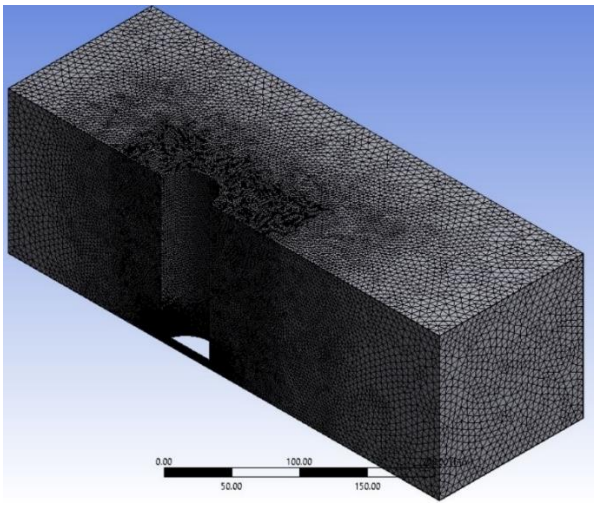

Fig. (4) Meshing of the fluid domain with the modification and the refinement zones

4. Mathematical model

In present work, the flow is assumed to be incompressible because of the low range of speeds compared to the speed of sound at the conditions used. Steady flow is considered as well although unsteady flow behavior of the vortex was observed by [3, and 12] but it is not the purpose of current study.

The Reynolds Averaged Navier-Stokes (RANS) equations of conservation of mass and momentum in the case of incompressible and steady flow can be written in Cartesian x,y,z coordinates as:

Mass conservation

$$\frac{\partial u}{\partial x}+\frac{\partial v}{\partial y}+\frac{\partial w}{\partial z}=0 \qquad (1)$$

x-momentum

$$u\frac{\partial u}{\partial x}+v\frac{\partial u}{\partial y}+w\frac{\partial u}{\partial z}=g_x-\frac{1}{\rho}\frac{\partial p}{\partial x}+\frac{\partial}{\partial x}\left\{-\overline{u'u'}+\nu\frac{\partial u}{\partial x}\right\}+\frac{\partial}{\partial y}\left\{-\overline{u'v'}+\nu\frac{\partial v}{\partial x}\right\}+\frac{\partial}{\partial z}\left\{-\overline{u'w'}+\nu\frac{\partial w}{\partial x}\right\} \qquad (2)$$

y-momentum

$$u\frac{\partial v}{\partial x}+v\frac{\partial v}{\partial y}+w\frac{\partial v}{\partial z}=g_y-\frac{1}{\rho}\frac{\partial p}{\partial y}+\frac{\partial}{\partial x}\left\{-\overline{v'u'}+\nu\frac{\partial u}{\partial y}\right\}+\frac{\partial}{\partial y}\left\{-\overline{v'v'}+\nu\frac{\partial v}{\partial y}\right\}+\frac{\partial}{\partial z}\left\{-\overline{v'w'}+\nu\frac{\partial w}{\partial y}\right\} \qquad (3)$$

z-momentum

$$u\frac{\partial w}{\partial x}+v\frac{\partial w}{\partial y}+w\frac{\partial w}{\partial z}=g_z-\frac{1}{\rho}\frac{\partial p}{\partial z}+\frac{\partial}{\partial x}\left\{-\overline{w'u'}+\nu\frac{\partial u}{\partial z}\right\}+\frac{\partial}{\partial y}\left\{-\overline{w'v'}+\nu\frac{\partial v}{\partial z}\right\}+\frac{\partial}{\partial z}\left\{-\overline{w'w'}+\nu\frac{\partial w}{\partial z}\right\} \qquad (4)$$

The Reynolds stress terms are calculated as reported by Menter [13] using k-ω SST, which is recommended by Liu et al. [14] to be more suitable for vortex flow.

5. Results

First of all, the proposed computational model is qualitatively validated against the experimental results of Kang et al. [9] who studied the HSV upstream of a 50 mm diameter cylinder experimentally using PIV technique. At Re_D=2*10e+4 (Re_D: Reynolds number based on the cylinder diameter) which corresponds to a free stream velocity of U∞= 5.76 m/s. The HSV structures are very close to one another as illustrated in Fig.(5).

In order to show the SHV intensity, most of the results are mainly u-velocity component distribution along the red vertical line shown in Fig. (3).

(a) Experimental measurements of [9]

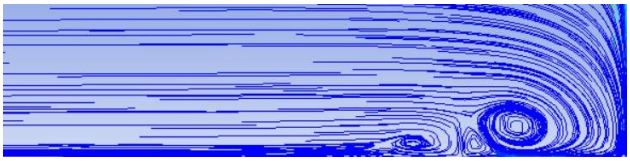

(b) Present simulation results

Fig. (5) Comparison between the experimental measurements of Kang et al. [9] and present simulation results.

5.1 Effect of free-stream velocity on HSV intensity: case of a cylinder without a hole

The HSV structure and intensity in case of a cylinder without a hole is dependent on Re_D to a great extent as illustrated in Figs. (6) to (10).

In Figs. (6) to (10) the variations of u-velocity component along the locus shown in Fig. (3) at free stream velocities of 10, 20, 30, 40, 50 m/s are shown. The peak negative u-component values are 0.7, 5.0, 10.0, 12.5 and 16.5 respectively. It is observed that circulation took place at all velocities, and the strength of the HSV, which is indicated by the magnitude of the negative u-velocity component, increases with increasing the free stream velocity and consequently Re_D. This is physically acceptable as when Re_D increases the stagnation pressure distribution along the vertical direction of the cylinder changes, so that the difference between the minimum value at the corner of the junction (which is equal to the static pressure as the velocity is zero because of the No-slip condition) and the maximum value at the free stream part of the cylinder is larger and so the HSV intensity is higher.

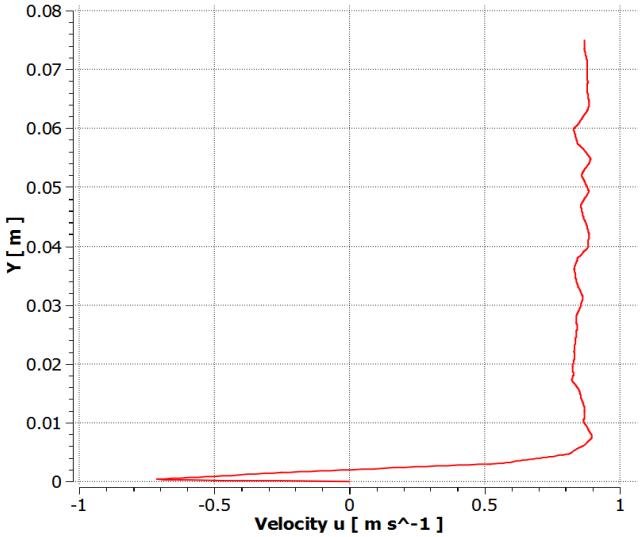

Fig. (6) Variation of u-velocity component at a free stream velocity of 10 m/s

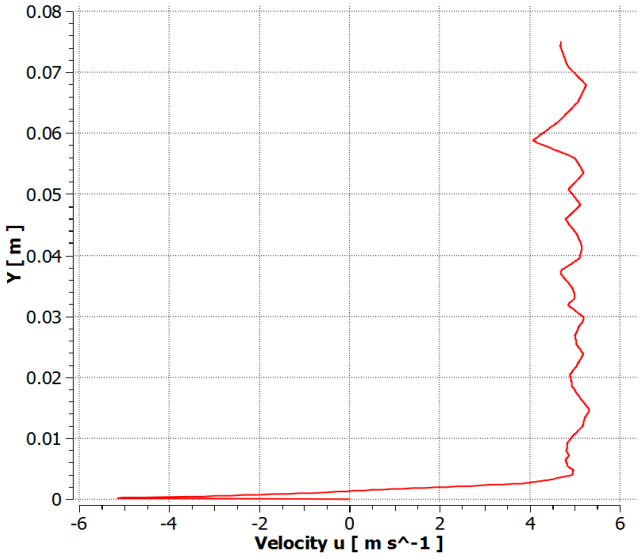

Fig. (7) Variation of u-velocity component at a free stream velocity of 20 m/s

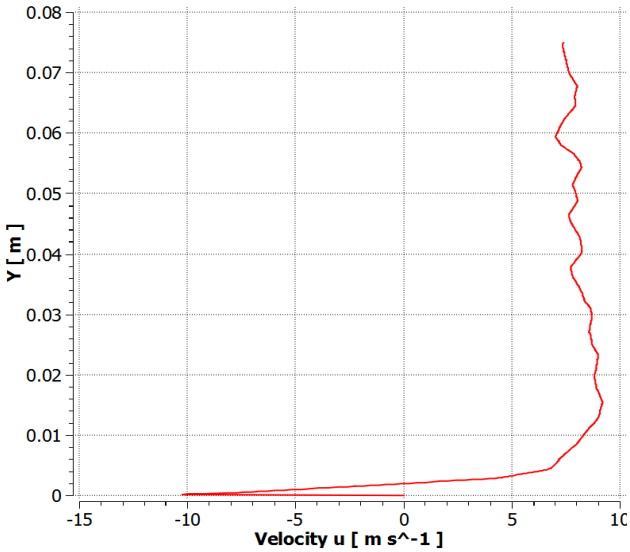

Fig. (8) Variation of u-velocity component at a free stream velocity of 30 m/s

5.2 Effect of hole height on the HSV structure

The structure of the HSV at constant free stream velocity of 50 m/s is studied at hole heights of 3 mm, 5 mm and 10 mm.

As for the 3 mm hole, it is observed in Fig. (11) that there is still a negative u-velocity in an amount of about 12 m/s which indicates that recirculation is still there. To assess the effect of the hole, the shape of the vortex in case of 3 mm hole and without the hole should be compared.

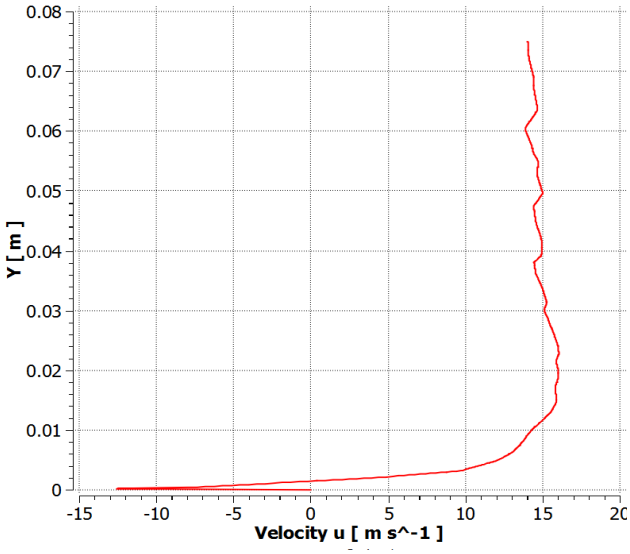

Fig. (9) Variation of u-velocity component at a free stream velocity of 40 m/s

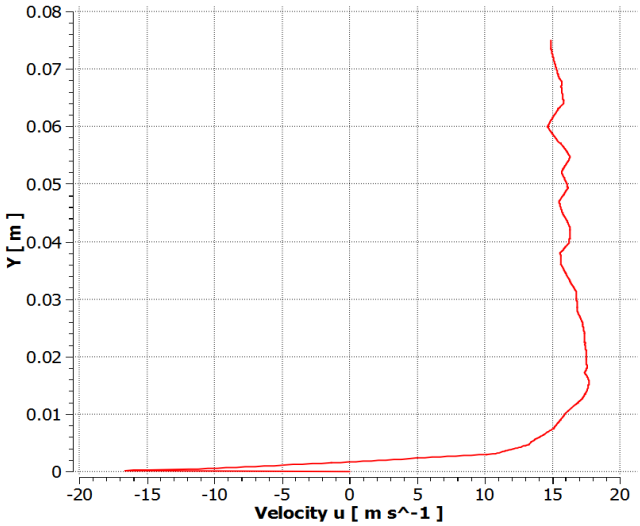

Fig. (10) Variation of u-velocity component at a free stream velocity of 50 m/s

In Fig. (12) the HSV structure at 50 m/s free stream velocity without a hole is shown. Half of the HSV can be seen clearly surrounding half of the cylinder. However, Fig. (13) shows the HSV structure in case of 3 mm height hole. Qualitatively speaking, the structure of HSV in the case without a hole is far more complex than the case with the 3 mm hole, and in the case of 3 mm hole, a considerable portion of the HSV is sucked passively to the downstream side of the cylinder.

Regarding the 5 mm and 10 mm height holes, the u-velocity component variations at the same location as previous cases are shown in Figs. (14) and (15). The figures show that the u-velocity component is never below zero, which means that recirculation did not take place, i.e. the HSV is completely sucked and eliminated.

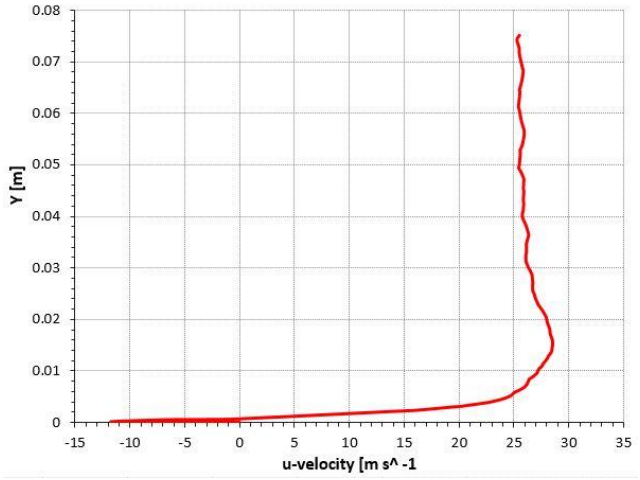

Fig. (11) U-velocity component in case of 3 mm hole and free stream velocity of 50 m/s

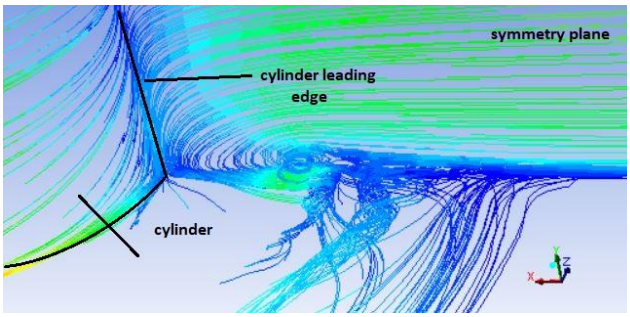

Fig. (12) Pathlines without a hole at free stream velocity of 50 m/s

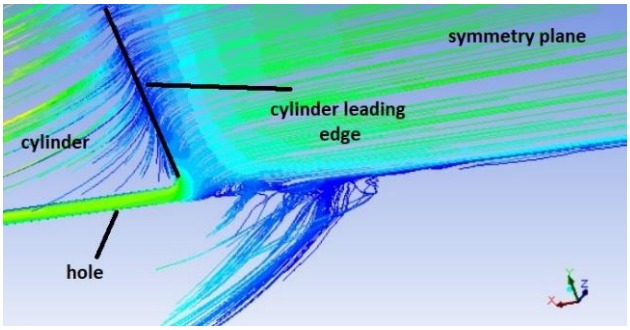

Fig. (13) Pathlines with 3 mm hole at free stream velocity of 50 m/s

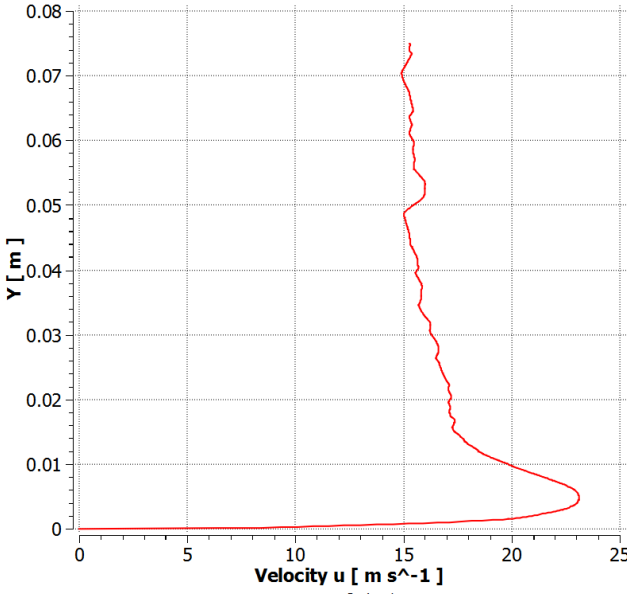

Fig. (14) U-velocity component in case of 5 mm hole and free stream velocity of 50 m/s

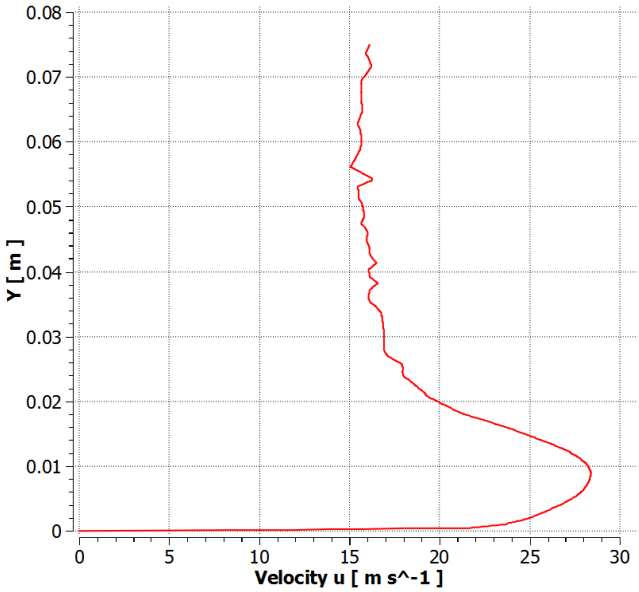

Fig. (15) U-velocity component in case of 10 mm hole and free stream velocity of 50 m/s

5. Conclusions

Numerical investigation of the structure of HSV with and without junction holes is carried out. From the above results, the following conclusions are made:

1. The strength of the HSV is mainly dependent on Re_D.
2. As Re_D increases the negative u-velocity component increases and so the HSV strength.
3. In case of 3 mm hole height, the HSV is partially eliminated.
4. In case of 5 mm and 10 mm heights the HSV vortex is completely sucked from the upstream to the downstream of the cylinder.

6. Nomenclature

BL	Boundary layer (the portion of the flow field near walls)
g	Acceleration of gravity, (m/s^2)
HSV	Horse-Shoe Vortex
p	Pressure (Pa)
Re_D	Reynolds number based on cylinder diameter
u,v,w	velocity components in x,y and z coordinate directions respectively, (m/s)
u′,v′,w′	velocity fluctuation components in x,y and z coordinate directions respectively, (m/s)
U∞	Free stream velocity (away from the boundary layer) (m/s)
x,y,z	Cartesian coordinates, (m)
ν	kinematic viscosity of air, (m^2/s)
ρ	air density , (kg/m^3)

7. References

[1] C. Baker, "The turbulent horseshoe vortex", Journal of Wind Engineering and Industrial Aerodynamics, Vol. 6, no. 1-2, pp. 9-23, 1980.

[2] A. Jacobi and R. Shah, "Heat transfer surface enhancement through the use of longitudinal vortices: A review of recent progress", Experimental Thermal and Fluid Science, Vol. 11, no. 3, pp. 295-309, 1995.

[3] F. Ballio, C. Bettoni and S. Franzetti, "A Survey of Time-Averaged Characteristics of Laminar and Turbulent Horseshoe Vortices", Journal of Fluids Engineering, Vol. 120, no. 2, p. 233, 1998.

[4] Kashyap, U., Das, K., and Debnath, B., "Effect of surface modification of a rectangular vortex generator on heat transfer rate from a surface to fluid: An extended study", International Journal of Thermal Sciences, Vol. 134, pp. 269-281, 2018.

[5] R. Simpson, "JUNCTIONFLOWS", Annual Review of Fluid Mechanics, Vol. 33, no. 1, pp. 415-443, 2001.

[6] W. Devenport and R. Simpson, "Time-dependent and time-averaged turbulence structure near the nose of a wing-body junction", Journal of Fluid Mechanics, Vol. 210, no. -1, p. 23, 1990.

[7] W. Devenport, N. Agarwal, M. Dewitz, R. Simpson and Poddar, "Effects of a fillet on the flow past a wing-body junction", AIAA Journal, Vol. 28, no. 12, pp. 2017-2024, 1990.

[8] L. Kubendran, H. Mcmahon and J. Hubbartt, "Turbulent flow around a wing/fuselage-type juncture", AIAA Journal, Vol. 24, no. 9, pp. 1447-1452, 1986.

[9] K. Kang, T. Kim and S. Song, "Strengths of horseshoe vortices around a circular cylinder with an upstream cavity", Journal of Mechanical Science and Technology, Vol. 23, no. 7, pp. 1773-1778, 2009.

[10] D. Philips, J. Cimbala and A. Treaster, "Suppression of the wing-body junction vortex by body surface suction", Journal of Aircraft, Vol. 29, no. 1, pp. 118-122, 1992.

[11] D. Barberis, P. Molton and T. Malaterre, "Control of 3D turbulent boundary layer separation caused by a wing–body junction", Experimental Thermal and Fluid Science, Vol. 16, no. 1-2, pp. 54-63, 1998.

[12] Toda, K., Haraoka, T., Sadahiro, T., and Yamada, H., "Unsteady Behavior of Necklace Vortex Produced by a Square Plate Protrusion", Open Journal of Fluid Dynamics, 08(01), pp. 59-72, 2018.

[13] F. Menter, "Two-equation eddy-viscosity turbulence models for engineering applications", AIAA Journal, Vol. 32, no. 8, pp. 1598-1605, 1994.

[14] Liu, J., Hussain, S., Wang, L., Xie, G., and Sundén, B., "Effects of a pocket cavity on heat transfer and flow characteristics of the endwall with a bluff body in a gas turbine engine", Applied Thermal Engineering, Vol. 143, pp. 935-946, 2018.